HTML ABSTRACT + LINKS

ARTICLES

Calculation of current densities using gauge-including atomic orbitals

Jonas Jusélius and Dage Sundholm[a)]
Department of Chemistry, P.O. Box 55 (A.I. Virtasen Aukio 1), FIN-00014 University of Helsinki, Helsinki, Finland

Jürgen Gauss[b)]
Institut für Physikalische Chemie, Universität Mainz, Jakob-Welder Weg 11, D-55099 Mainz, Germany

(Received 26 March 2004; accepted 24 May 2004)

A method for calculating the various components of the magnetically induced current-density tensor using gauge-including atomic orbitals is described. The method is formulated in the framework of analytical derivative theory, thus enabling implementation at the Hartree–Fock self-consistent-field (HF-SCF) as well as at electron-correlated levels. First-order induced current densities have been computed up to the coupled-cluster singles and doubles level (CCSD) augmented by a perturbative treatment of triple excitations [CCSD(T)] for carbon dioxide and benzene and up to the full coupled-cluster singles, doubles, and triples (CCSDT) level in the case of ozone. The applicability of the gauge including magnetically induced current method to larger molecules is demonstrated by computing first-order current densities for porphin and hexabenzocoronene at the HF-SCF and density-functional theory level. Furthermore, a scheme for obtaining quantitative values for the induced currents in a molecule via numerical integration over the current flow is presented. For benzene, a perpendicular magnetic field induces a (field dependent) ring current of 12.8 nA T^{-1} at the HF-SCF level using a triple-zeta basis set augmented with polarization functions (TZP). At the CCSD(T)/TZP level the induced current was found to be 11.4 nA T^{-1}. Gauge invariance and its relation to charge-current conservation is discussed. © *2004 American Institute of Physics*. [DOI: 10.1063/1.1773136]

I. INTRODUCTION

The current density induced in the molecular electron density by an external magnetic field is invariant under gauge transformations. In quantum chemical calculations of magnetic properties, however, the issue of gauge invariance is usually limited to the discussion of gauge-origin independence, i.e., the transformation properties with respect to a special class of gauge transformations. Most of the so far reported calculations of magnetically induced current densities do not satisfy gauge-origin independence due to the use of finite basis sets in the same manner as corresponding calculations of nuclear magnetic shielding constants. The use of gauge-including atomic orbitals (GIAO), also known as London orbitals, represents one, and in our opinion the most elegant possibility to resolve the gauge-origin problem in nuclear magnetic shielding calculations.[1–24] By employing explicitly magnetic-field-dependent basis functions the gauge-origin dependence of calculated nuclear magnetic shielding constants as well as other magnetic properties can be eliminated.[2] The idea to use field-dependent basis functions to remove the gauge-origin dependence can be traced back to the work of London.[3] It was first used in nuclear magnetic shielding calculations by Hameka[4] and later by Ditchfield and others.[5,21,22] However, the actual breakthrough of the GIAO approach is due to the work of Wolinski *et al.*,[6,7] who demonstrated that modern analytic derivative theory[25] can be efficiently used for the calculation of nuclear magnetic shieldings within the GIAO framework. The GIAO approach has since then been implemented in most of the popular quantum chemical program systems[8–11] and also extended to computational levels beyond the Hartree–Fock level.[8,10–20,23]

Even though the use of GIAOs is currently the most popular approach to resolve the gauge-origin issue in shielding calculations,[1] magnetically induced current densities are in most cases still obtained using computational methods with an explicit gauge-origin dependence.[26,27] Recently, the continuous transformation of current-density (CTOCD) approach[26–36] has become available for computing induced current densities. In this approach, the gauge-origin problem is resolved by using a different gauge origin for each point for which the current density is calculated. Within the CTOCD-DZ variant the gauge origin is identical to the point at which the current density is computed,[30,31] while in the CTOCD-PZ variant the gauge origin is chosen such that the transverse component of the paramagnetic current density is annihilated.[32–34] Improved CTOCD approaches obtained by shifting the gauge origin have also been suggested.[28,29,33,34] Experience with nuclear magnetic shieldings, however, indicates that the CTOCD schemes generally are less efficient

[a)]Electronic mail: jonas@chem.helsinki.fi, sundholm@chem.helsinki.fi
[b)]Electronic mail: gauss@mail.uni-mainz.de

 © 2004 American Institute of Physics

Downloaded 19 Aug 2004 to 128.146.233.123. Redistribution subject to AIP license or copyright, see http://jcp.aip.org/jcp/copyright.jsp

than the GIAO approach for computing magnetic properties.[37]

In this article, we present a new computational approach to calculate magnetically induced current densities based on GIAOs and analytical derivative theory. Due to the use of GIAOs, no reference to the gauge origin appears in the final expression for the first-order induced current density. The obtained currents are gauge-origin independent but gauge invariance is achieved only in the limit of complete basis set. The derivation is based on the Biot–Savart expression for the nuclear magnetic shielding tensor[26,30,38] as well as the corresponding expressions obtained within analytic derivative theory.[6,10,12–14,17] The resulting expression is cast in a form which only requires knowledge about the unperturbed and perturbed one-electron density matrices. Current densities can thus be calculated within the present approach at all computational levels for which these one-electron density matrices are available. The presented scheme is applied to carbon dioxide (CO_2), ozone (O_3), and benzene (C_6H_6) at various electron-correlated quantum chemical levels as well as to large molecular systems such as porphin ($C_{20}N_4H_{14}$) and hexabenzocoronene ($C_{42}H_{18}$) at the Hartree–Fock self-consistent-field (HF-SCF) and density-functional-theory level.

In an external magnetic field, aromatic and anti-aromatic molecules sustain induced ring currents whose strength can be used as a measure for the degree of aromaticity (anti-aromaticity).[39,40] The induced ring current leads to an additional (induced) magnetic field that can be observed as a long-range magnetic shielding contribution. In our previous work,[41–47] we estimated ring-current strengths from the shape of the long-range magnetic shielding function based on Biot–Savart's law for an infinitely thin and circular conductor. In the present paper, we obtain the ring-current strengths for benzene, porphin, and hexabenzocoronene directly via explicit numerical integration over the net current flow through one of the bond cross sections within the considered molecular ring. This approach has the advantage that current strengths can also be obtained for molecules with complex connected ring structures (such as, for example, in the case of hexabenzocoronene) and thus provides a detailed and quantitative magnetic measure of aromaticity.

II. THEORY

A. The current density

In the presence of a uniform, time-independent magnetic field with a flux **B**, a current density **J** is induced within the molecular electron density:

$$\mathbf{J}(\mathbf{r}) = \frac{i}{2}\int d\mathbf{r}_2 \ldots d\mathbf{r}_n (\Psi^* \boldsymbol{\nabla}\Psi - \Psi\boldsymbol{\nabla}\Psi^* + 2i\mathbf{A}\Psi^*\Psi). \tag{1}$$

In Eq. (1), Ψ is the wave function, and **A** is the vector potential describing both the external magnetic field and the magnetic fields arising from the nuclei in a molecule

$$\mathbf{A}(\mathbf{r}) = \mathbf{A}^{\mathbf{B}}(\mathbf{r}) + \sum_I^N \mathbf{A}^{\mathbf{m}_I}(\mathbf{r}) \tag{2}$$

with

$$\mathbf{A}^{\mathbf{B}}(\mathbf{r}) = \tfrac{1}{2}\mathbf{B}\times(\mathbf{r}-\mathbf{R}_O) \tag{3}$$

and

$$\mathbf{A}^{\mathbf{m}_I}(\mathbf{r}) = \alpha^2 \frac{\mathbf{m}_I \times (\mathbf{r}-\mathbf{R}_I)}{|\mathbf{r}-\mathbf{R}_I|^3}. \tag{4}$$

In the given equations, $\mathbf{R}_O$ represents the chosen gauge origin of the magnetic field, $\mathbf{m}_I$ the nuclear magnetic moment of the Ith nucleus and $\mathbf{R}_I$ the position of this nucleus, and α is the fine-structure constant. Atomic units are used in this work. In an isolated system charge conservation holds, i.e., charge cannot be created nor destroyed. For a molecule in a stationary state the charge-conservation condition becomes $\boldsymbol{\nabla}\cdot\mathbf{J}=0$. For closed-shell molecules in the absence of an external magnetic field, this reduces to $\mathbf{J}=0$.

In an isotropic medium, the magnetic flux density **B** is uniquely defined via the vector potential **A**. However, the reverse is not true since $\mathbf{B}=\boldsymbol{\nabla}\times(\mathbf{A}(\mathbf{r})+\boldsymbol{\nabla}\Phi(\mathbf{r})) = \boldsymbol{\nabla}\times\mathbf{A}(\mathbf{r})$. Here, $\Phi(\mathbf{r})$ stands for an arbitrary scalar function, thus rendering the choice of the gauge (or more specifically the gauge origin $\mathbf{R}_O$) for a magnetic field undetermined. While gauge-invariance holds for the exact solution of the Schrödinger equations and also for some approximate solutions when using a complete one-particle basis set,[48] the use of finite one-particle basis sets unavoidably introduces a gauge-dependence in quantum chemical calculations of magnetic properties. A number of different approaches exist to remedy this problem.[3–7,49,50] None of these approaches accomplish true gauge invariance but rather gauge-origin independence. In the present work, gauge-origin independence is obtained by using GIAOs,

$$\chi_\mu(\mathbf{r}) = e^{-(i/2)(\mathbf{B}\times[\mathbf{R}_\mu-\mathbf{R}_O]\cdot\mathbf{r})}\chi_\mu^{(0)}(\mathbf{r}). \tag{5}$$

In Eq. (5), $\chi_\mu^{(0)}(\mathbf{r})$ denotes a standard Gaussian-type basis function with $\mathbf{R}_\mu$ as center and $\mathbf{R}_O$ as the chosen gauge origin. The use of GIAOs eliminates all explicit reference to the (global) gauge origin $\mathbf{R}_O$ in the corresponding expressions and in addition it ensures rapid basis-set convergence for the corresponding second-order magnetic properties.

B. Analytic derivative based current-density theory

The electronic energy of a molecular system can generally be written in terms of density matrices as

$$E = \sum_{\mu\nu} h_{\mu\nu}D_{\mu\nu} + \frac{1}{2}\sum_{\mu\nu\sigma\rho} g_{\mu\sigma\nu\rho}d_{\mu\sigma\nu\rho}, \tag{6}$$

where $h_{\mu\nu}$ and $g_{\mu\sigma\nu\rho}$ are the one- and two-electron interaction integrals,

$$h_{\mu\nu} = \int d\mathbf{r}\chi_\mu^*\hat{\mathbf{h}}\chi_\nu,$$

$$g_{\mu\sigma\nu\rho} = \int\int d\mathbf{r}_1 d\mathbf{r}_2 \chi_\mu^*\chi_\sigma^* r_{12}^{-1}\chi_\nu\chi_\rho, \tag{7}$$

$D_{\mu\nu}$ and $d_{\mu\sigma\nu\rho}$ the one- and two-electron density matrices in the atomic-orbital representation, and $\hat{\mathbf{h}}$ the one-electron Hamiltonian. To derive a derivative-theory-based expression for the magnetically induced current density, we start from

Downloaded 19 Aug 2004 to 128.146.233.123. Redistribution subject to AIP license or copyright, see http://jcp.aip.org/jcp/copyright.jsp

the corresponding derivative expression for the nuclear magnetic shielding tensor that is obtained by differentiating the total energy in Eq. (6) with respect to the nuclear magnetic moments and the components of the external magnetic field in the limit of zero magnetic field:

$$\sigma^I_{\alpha\beta}=\left.\frac{\partial^2 E}{\partial m^I_\alpha \partial B_\beta}\right|_{\substack{\mathbf{B}=0\\ \mathbf{m}_I=0}}. \tag{8}$$

Evaluating Eq. (8) via the energy expression in Eq. (6) yields the following expression for the magnetic shielding tensor elements;

$$\sigma^I_{\alpha\beta}=\sum_{\mu\nu} D_{\mu\nu}\frac{\partial^2 h_{\mu\nu}}{\partial m^I_\alpha \partial B_\beta}+\sum_{\mu\nu}\frac{\partial D_{\mu\nu}}{\partial B_\beta}\frac{\partial h_{\mu\nu}}{\partial m^I_\alpha} \tag{9}$$

with $\partial D_{\mu\nu}/\partial B_\beta$ as the magnetically perturbed density matrices and $\partial h_{\mu\nu}/\partial m^I_\alpha$ as well as $\partial^2 h_{\mu\nu}/\partial m^I_\alpha \partial B_\beta$ as the corresponding derivatives of the integrals of $\hat{\mathbf{h}}$ in the AO representation.

On the other hand, the second-order interaction energy due to the interaction of nuclear magnetic moments with an external magnetic field can also be given in terms of the current density and the vector potential due to the corresponding nuclear magnetic moment,[26]

$$E^{mB}=-\int \mathbf{A}^{\mathbf{m}_I}(\mathbf{r})\cdot\mathbf{J}^{\mathbf{B}}(\mathbf{r})d\mathbf{r}. \tag{10}$$

Evaluation of the second derivative in Eq. (8) using Eq. (10) yields an alternative expression for the nuclear magnetic shielding tensor

$$\sigma^I_{\alpha\beta}=-\epsilon_{\alpha\delta\gamma}\int\frac{(r_\delta-R_{I\delta})}{|\mathbf{r}-\mathbf{R}_I|^3}\mathcal{J}^{B\beta}_\gamma d\mathbf{r}, \tag{11}$$

where

$$\mathcal{J}^{B\beta}_\gamma(\mathbf{r})=\frac{\partial J_\gamma(\mathbf{r})}{\partial B_\beta} \tag{12}$$

are the tensor elements of the first-order induced current density, and $\epsilon_{\alpha\delta\gamma}$ is the Levi-Civita tensor. Equating Eqs. (9) and (11) and explicitly introducing the one-electron basis functions, we obtain the following equation that relates nuclear magnetic shieldings and the current-density tensor:

$$\begin{aligned}&\int\sum_{\mu\nu} D_{\mu\nu}\frac{\partial^2}{\partial m^I_\alpha\partial B_\beta}\{\chi^*_\mu(\mathbf{r})\hat{h}\chi_\nu(\mathbf{r})\}d\mathbf{r}\\ &+\int\sum_{\mu\nu}\frac{\partial D_{\mu\nu}}{\partial B_\beta}\frac{\partial}{\partial m^I_\alpha}\{\chi^*_\mu(\mathbf{r})\hat{h}\chi_\nu(\mathbf{r})\}d\mathbf{r}\\ &=-\epsilon_{\alpha\delta\gamma}\int\frac{(r_\delta-R_{I\delta})}{|\mathbf{r}-\mathbf{R}_I|^3}\mathcal{J}^{B\beta}_\gamma(\mathbf{r})d\mathbf{r}.\end{aligned} \tag{13}$$

It can easily be seen from the general expression for the magnetic interaction energy E^{mB} that the integrands on the left- and right-hand sides of Eq. (13) must be identical. In order to determine $\mathcal{J}^{B\beta}_\gamma(\mathbf{r})$ in discrete space points we drop the integral signs on both sides in Eq. (13). Together with the use of field-dependent basis functions [Eq. (5)] this yields

$$\begin{aligned}-\epsilon_{\alpha\delta\gamma}\frac{(r_\delta-R_{I\delta})}{|\mathbf{r}-\mathbf{R}_I|^3}\mathcal{J}^{B\beta}_\gamma(\mathbf{r})&=\sum_{\mu\nu}\frac{\partial D_{\mu\nu}}{\partial B_\beta}\chi^*_\mu(\mathbf{r})\frac{\partial\hat{h}}{\partial m^I_\alpha}\chi_\nu(\mathbf{r})\\ &+\sum_{\mu\nu}D_{\mu\nu}\frac{\partial\chi^*_\mu(\mathbf{r})}{\partial B_\beta}\frac{\partial\hat{h}}{\partial m^I_\alpha}\chi_\nu(\mathbf{r})\\ &+\sum_{\mu\nu}D_{\mu\nu}\chi^*_\mu(\mathbf{r})\frac{\partial\hat{h}}{\partial m^I_\alpha}\left\{\frac{\partial\chi_\nu(\mathbf{r})}{\partial B_\beta}\right\}\\ &+\sum_{\mu\nu}D_{\mu\nu}\chi^*_\mu(\mathbf{r})\frac{\partial^2\hat{h}}{\partial m^I_\alpha\partial B_\beta}\chi_\nu(\mathbf{r})\end{aligned} \tag{14}$$

with the derivatives of the one-electron Hamiltonian given by

$$\left.\frac{\partial\hat{h}}{\partial\mathbf{m}_I}\right|_{\substack{\mathbf{B}=0\\ \mathbf{m}_I=0}}=\alpha^2\frac{(\mathbf{r}-\mathbf{R}_I)\times\mathbf{p}}{|\mathbf{r}-\mathbf{R}_I|^3}, \tag{15}$$

$$\left.\frac{\partial^2\hat{h}}{\partial\mathbf{m}_I\partial\mathbf{B}}\right|_{\substack{\mathbf{B}=0\\ \mathbf{m}_I=0}}=\frac{\alpha^2}{2}\frac{[(\mathbf{r}-\mathbf{R}_O)\cdot(\mathbf{r}-\mathbf{R}_I)\mathbf{1}-(\mathbf{r}-\mathbf{R}_O)(\mathbf{r}-\mathbf{R}_I)]}{|\mathbf{r}-\mathbf{R}_I|^3}. \tag{16}$$

Although these operators explicitly depend on the gauge origin $\mathbf{R}_O$ and thus seem to render the first-order current tensor gauge dependent, it can be shown that the gauge-dependent terms cancel exactly against terms arising from the differentiation of the GIAOs.

Further simplifications of Eq. (14) yield the working equations for the calculation of the various components of the magnetically induced current-density tensor, $\mathcal{J}^{B\beta}_\alpha(\mathbf{r})$,

$$\begin{aligned}\mathcal{J}^{B\beta}_\alpha(\mathbf{r})&=\sum_{\mu\nu}D_{\mu\nu}\frac{\partial\chi^*_\mu(\mathbf{r})}{\partial B_\beta}\frac{\partial\tilde{h}}{\partial m^I_\alpha}\chi_\nu(\mathbf{r})\\ &+\sum_{\mu\nu}D_{\mu\nu}\chi^*_\mu(\mathbf{r})\frac{\partial\tilde{h}}{\partial m^I_\alpha}\frac{\partial\chi_\nu(\mathbf{r})}{\partial B_\beta}\\ &+\sum_{\mu\nu}\frac{\partial D_{\mu\nu}}{\partial B_\beta}\chi^*_\mu(\mathbf{r})\frac{\partial\tilde{h}}{\partial m^I_\alpha}\chi_\nu(\mathbf{r})\\ &-\epsilon_{\alpha\beta\delta}\left[\sum_{\mu\nu}D_{\mu\nu}\chi^*_\mu(\mathbf{r})\frac{\partial^2\tilde{h}}{\partial m^I_\alpha\partial B_\delta}\chi_\nu(\mathbf{r})\right],\end{aligned} \tag{17}$$

where we have defined a new set of operators, $\partial\tilde{h}/\partial m^I_\alpha$ and $\partial^2\tilde{h}/\partial m^I_\alpha\partial B_\delta$, without the denominator $|\mathbf{r}-\mathbf{R}_I|^3$. Note that Eq. (17) is easily evaluated at any space point, since it only involves basis functions and derivatives of basis functions at that point as well as the corresponding one-electron density matrices. It should be also noted that the explicit dependence of each individual contribution on the nuclear position $\mathbf{R}_I$ cancels out in the sum of all contributions, thus making the current-density tensor independent of the nuclear positions $\mathbf{R}_I$ and the magnetic moments m^I_α, as it should be.

It is also possible to derive an expression for $\mathcal{J}^{B\beta}_\alpha$ in terms of the corresponding expressions for the magnetizability tensor. Although such an approach might seem to be more natural, since the first-order current density is independent of

Downloaded 19 Aug 2004 to 128.146.233.123. Redistribution subject to AIP license or copyright, see http://jcp.aip.org/jcp/copyright.jsp

the nuclear magnetic moments, this approach leads to complications when working with GIAOs. Due to the magnetic-field dependence of GIAOs the generalized Hellmann–Feynman theorem cannot be as easily applied when evaluating Eq. (8) thus rendering that approach more involved.

C. Implementation details

In order to implement the given equations for $\mathcal{J}_{\alpha}^{B_\beta}(\mathbf{r})$ in a computer program, it is advantageous to recast Eq. (17) in a matrix-vector form. The starting point for such a form is a vector $\mathbf{v}$ whose vector elements consist of the basis-function values at each grid point $\mathbf{r}$. Furthermore, we need to evaluate the derivative values of the basis functions with respect to x, y, and z. Due to the explicit field dependence of the GIAOs we also need to evaluate the first derivative of the basis functions with respect to the components of the external magnetic field as well as a mixed second derivative with respect to $\mathbf{B}$ and x, y, and z. The vector expression for $\mathcal{J}_{\alpha}^{B_\beta}(\mathbf{r})$ is then given by

$$\boldsymbol{\mathcal{J}}_{\alpha}^{B_\beta}=\mathbf{v}^T\mathbf{P}_\beta\mathbf{d}_\alpha-\mathbf{b}_\beta^T\mathbf{D}\mathbf{d}_\alpha+\mathbf{v}^T\mathbf{D}\mathbf{q}_{\alpha\beta}-\epsilon_{\alpha\beta\gamma}\tfrac{1}{2}(\mathbf{v}^T\mathbf{D}\mathbf{v})\mathbf{r}_\gamma \tag{18}$$

with $\mathbf{D}$ as the AO density matrix, $\mathbf{P}_\alpha$ the perturbed AO density matrices, and the quantities $\mathbf{b}_\alpha$, $\mathbf{d}_\alpha$, $\mathbf{q}_{\alpha\beta}$ given by

$$\mathbf{b}_\alpha=\frac{\partial\mathbf{v}}{\partial\mathbf{B}_\alpha}, \tag{19}$$

$$\mathbf{d}_\alpha=\frac{\partial\mathbf{v}}{\partial\mathbf{r}_\alpha}\quad(\alpha,\beta=x,y,z), \tag{20}$$

$$\mathbf{q}_{\alpha\beta}=\frac{\partial^2\mathbf{v}}{\partial\mathbf{r}_\alpha\mathbf{B}_\beta}. \tag{21}$$

The density matrices $\mathbf{D}$ and $\mathbf{P}_\alpha$ are obtained from standard *ab initio* program packages capable of calculating nuclear magnetic shielding tensors.

D. Integration of current densities

Although the current density is a proper quantum mechanical observable, it has not been directly observed experimentally. As such, current-density maps can convey information about molecules, thus aiding the understanding of the current paths in the molecule. However, current-density plots do not provide any quantifiable measures of the current strengths nor are they suitable for comparing current strengths in different molecular systems. By integration over the current flow passing through specific bonds, it is possible to obtain the net current strengths around a molecular ring or through a bond. In noncyclic molecules, the net current flow, however, must be zero, in order for the law of charge conservation to hold.

The integration of the current density is carried out using two-dimensional Gaussian or Lobatto quadrature[51] over a bond cross section. The Gauss integration points x_i are given by the nodes of the Legendre polynomials $P_n(x)$, while the integration weights w_i^G are obtained from the differentiated polynomials,

$$\left(\frac{dP_n(x_i)}{dx}\right).$$

In one dimension, Gauss quadrature yields

$$\int_a^b f(x)dx=\sum_{k=1}^{m}\left(\sum_{i=1}^{n} w_i^G f_k(x_i)\right), \tag{22}$$

where the sum over k originates from the piecewise integration and f_k is the function f shifted to $[-1,1]$ on the kth interval. The integration weights are given by

$$w_i^G=\frac{2}{(1-x_i^2)}\left(\frac{dP_n(x_i)}{dx}\right)^2. \tag{23}$$

In the Lobatto integration, the integration points are determined via the nodes of the first derivative of the Legendre polynomials of order $n-1$,

$$\left(\frac{dP_{n-1}(x)}{dx}\right).$$

In addition, the function values at the end points of the interval are also considered in the Lobatto integration. The integration weights w_i^L are obtained from $P_{n-1}(x_i)$. The one-dimensional Lobatto quadrature then reads

$$\int_a^b f(x)dx=\sum_{k=1}^{m}\left(w_1^L f_k(-1)+w_n^L f_k(1)+\sum_{i=2}^{n-1} w_i^L f_k(x_i)\right) \tag{24}$$

with the corresponding weights given by

$$w_i^L=\frac{2}{n(n-1)(P_{n-1}(x_i))^2} \tag{25}$$

and the integration weights for the end points by

$$w_1^L=w_n^L=\frac{2}{n(n-1)}. \tag{26}$$

Numerical values for the integration points and weights are tabulated in Ref. 51.

Cyclic systems such as aromatic molecules can sustain a net current that flows around the molecular rings. The net current should be independent of where in the ring it is calculated. Due to practical issues, this is not necessarily always the case. In the numerical integration of the currents passing a given bond, one has to be careful where and how to cut the bond. The choice of grid and method of integration is by far less critical. For benzene, convergence of the integrated current is achieved with a grid that starts in the ring center, passes through the center of the bond, and is perpendicular to the molecular plane. The integration area has to be extended to about 5 bohr outside the bond and 5 bohr above and below the ring to incorporate the most significant part of the current flow. In principle, it does not matter where the bond cross section is positioned, but it is recommended to use cross sections containing the bond midpoint. The reason is that in the vicinity of the nuclei, the current-density vector field can be rather strong and thus render integration more difficult. Dense grids are then needed to converge the integrals, while for integrations over bond cross sections containing the bond midpoint as few as 20 grid points in each direction are often

Downloaded 19 Aug 2004 to 128.146.233.123. Redistribution subject to AIP license or copyright, see http://jcp.aip.org/jcp/copyright.jsp

sufficient for obtaining accurate integral values. The divergence problem discussed in Sec. II E also suggests that the integration plane is chosen as far away from the nuclei as possible.

For noncyclic molecules (e.g., carbon dioxide, ozone) the net current is necessarily zero. In spite of this, it is still possible to obtain the strength of the current in individual bonds by splitting the integral into positive and negative contributions, or alternatively, integrating over only half of the bond cross section. Currents obtained in such a way are however dependent on the location of the cut-plane. Such ''bond currents'' might prove useful as some kind of measure of electron delocalization.

E. The divergence of the current

As mentioned earlier, the current obeys the law of charge conservation, i.e., the divergence of the current must be zero in *every* point of space. This requirement holds for time-independent systems. For time-dependent systems, the divergence must be equal to a corresponding change of the density at time t. Alternatively, the law of charge conservation can be viewed as a consequence of gauge invariance.[52] Thus, if true gauge invariance is not achieved, the calculated current will to some extent be divergent. Epstein has showed that the use of GIAOs does not necessarily lead to the expected current conservation[52] even though the magnetic shielding tensor is gauge-origin independent. This is not surprising, since the GIAO approach can be viewed as a recipe for the unique definition of a set of local gauge-origins for the basis functions. Gauge-origin dependence is in this way eliminated, but gauge invariance cannot achieved in this manner. The use of GIAOs significantly improve basis-set convergence toward gauge invariant results at the basis-set limit, in particular for nuclear magnetic shielding tensors.

By calculating the divergence of the current ($\nabla \cdot \mathbf{J}(r)$) in selected points of space, one can obtain a measure of the gauge-invariance errors, and thus of the basis-set completeness. In our code, the divergence is calculated by using a five point formula for numerical differentiation on a locally tight, three-dimensional grid. The law of charge conservation can alternatively be expressed using the Sambe–Epstein integral condition for charge-current conservation[26]

$$\int \mathbf{J}(\mathbf{r})\, d\mathbf{r} = 0. \tag{27}$$

For molecules with a center of inversion this integral is for symmetry reasons equal to zero, whereas for general molecules, Eq. (27) is fulfilled only when the charge is conserved.

III. COMPUTATIONAL DETAILS

First-order induced current densities have been computed for carbon dioxide (CO_2), ozone (O_3), and benzene (C_6H_6) at Hartree–Fock self-consistent-field (HF-SCF) and density-functional theory (DFT) levels using the above theory as implemented in the program GIMIC. The current densities at the DFT level are obtained within the usual assumption that the exchange-correlation functional depends only on the electron density, since DFT studies indicated that current-density functionals are so far unable to provide an improved description of the magnetic perturbations.[18] The induced current densities for CO_2, O_3, and C_6H_6 have also been studied at various coupled-cluster (CC) levels such as CC singles and doubles (CCSD) and CCSD augmented by a perturbative treatment of triple excitations [CCSD(T)]. For O_3, additional calculations at the full CC singles, doubles, triples (CCSDT) level have been performed. All calculations have been carried out using equilibrium geometries optimized at the CCSD(T) level using Dunning's correlation-consistent polarized valence quadruple-zeta (cc-pVQZ) basis.[53]

For CO_2, the basis-set convergence was checked at different levels of theory by performing calculations with increasing size of the basis set. The following sets that have already proven useful in shielding calculations have been used: split-valence plus polarization (SVP), triple-zeta single and double polarization (TZP and TZ2P), quadruple-zeta double polarization (QZ2P), and a polarized near pentuple-zeta quality basis (PZ3D2F).[54,55] In the study of charge conservation, Dunning's pentuple-zeta (cc-pV5Z) basis sets were used.[53,56]

The molecular structures of porphin ($C_{20}N_4H_{14}$) and hexabenzocoronene ($C_{42}H_{18}$) have been obtained at the resolution-of-identity density-functional-theory (RI-DFT) level[57] using the Becke–Perdew (BP86) functional[58–60] together with the SVP basis set. In the current-density calculations on $C_{42}H_{18}$, a triple-zeta quality basis sets augmented by polarization functions (TZP) were employed,[55] whereas in the current-density calculations on porphin we used triple-zeta valence basis sets augmented by polarization functions (TZVP).[61]

Calculations of the unperturbed and perturbed density matrices have been performed using the Mainz-Austin-Version of the ACES II program package[62] (MP2 and CC calculations) as well as the TURBOMOLE program package[55] (HF-SCF and DFT calculations).

IV. RESULTS

A. Carbon dioxide

Carbon dioxide (CO_2) is a fairly simple molecule whose current density has previously been studied by Zanasi *et al.*[26,32] A visual comparison of the current density for CO_2 calculated at the HF-SCF level with the corresponding current density reported in Ref. 32 shows that the two independent approaches provide essentially identical current densities. In Fig. 1(a), the magnitude (modulus) of the first-order induced current density is shown. The displayed current density is calculated in a plane containing the nuclei with the external magnetic field perpendicular to the plane. In Fig. 1(b), the current vectors projected onto the plane are shown. The vectors have been obtained by contracting the current-density tensor $\mathcal{J}_{\alpha}^{B\beta}(\mathbf{r})$ with the applied external magnetic field.

The basis-set study shows that the calculated current density is rather basis-set independent. Since one hardly can see any differences in the plotted current densities calculated

Downloaded 19 Aug 2004 to 128.146.233.123. Redistribution subject to AIP license or copyright, see http://jcp.aip.org/jcp/copyright.jsp

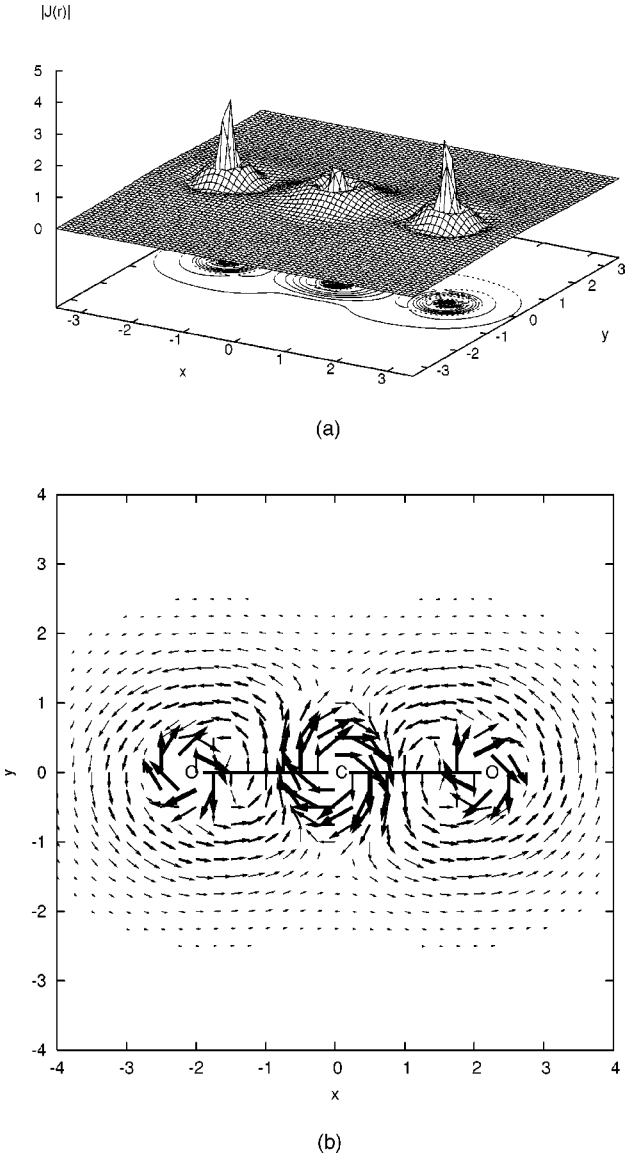

FIG. 1. The magnitude (a) and direction (b) of the induced current density (in a.u.) calculated in the molecular plane of CO_2 at the HF-SCF/TZP level.

with different basis sets, the integrated current strength is used to illustrate the convergence. The reported strengths have been obtained by numerical integration over half of the bond cross section (note that the full integration yields a vanishing current strength) containing the midpoint of the CO bond. In the basis-set study, we considered the SVP, TZP, TZ2P, QZ2P, PZ3D2F, and cc-pV5Z sets. Although these sets have not been constructed in a systematic manner, the experience is that they work rather well for magnetic properties. As seen in Fig. 2, the current strength decreases monotonously by about 3% when increasing the basis-set size from SVP to PZ3D2F. The only exception is the current density obtained using the TZ2P basis sets. The integrated currents obtained with the TZ2P basis set are somewhat larger than those calculated using the TZP, QZ2P, and PZ3d2F basis sets; the TZ2P basis set seems to be somewhat unbalanced compared to the other basis sets employed.

Electron-correlation effects on the current density of CO_2 have been investigated by performing MP2, CCSD, CCSD(T), and DFT calculations. As one might expect, the electron-correlation contributions to the current density of CO_2 are found to be small. The basis-set dependence of the integrated current calculated at the different levels of theory is shown in Fig. 2. The electron correlation reduces the integrated current strength for CO_2 by roughly 6%. Since both basis-set errors and electron-correlation corrections decrease the induced current, the current strength calculated at the CCSD(T)/PZ3D2F level is about 9% smaller than the corresponding HF-SCF/SVP value.

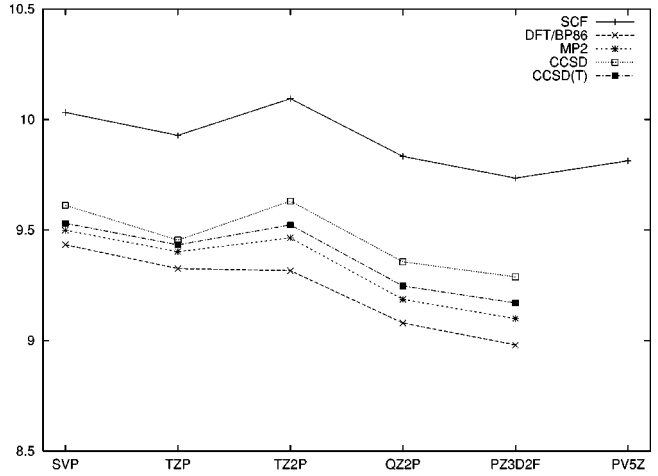

FIG. 2. The basis-set convergence for the induced current (in $nA\,T^{-1}$) calculated at the HF-SCF, DFT-BP86, MP2, CCSD, and CCSD(T) levels for CO_2.

B. Benzene

Benzene is the classic example of an aromatic molecule. The criteria often used for aromaticity are low reactivity, planar structure, energetic stability, proton chemical shifts, and magnetic susceptibility anisotropy.[63] The concept of aromaticity has also been extended to molecules that deviate (slightly) from planarity such as homoaromatic molecules,[47] and even to three-dimensional molecules.[64]

The reason for the large magnetic susceptibility anisotropy is the strong ring current in the molecular frame induced by the external magnetic field. The strength of the ring current is today a generally accepted measure of aromaticity.[3,26,39,50,65–72] We have previously estimated the strength of the induced ring current by applying our aromatic ring-current shielding (ARCS) method.[41] Using this method, a ring-current strength of 8.0 $nA\,T^{-1}$ was estimated for benzene from the long-range magnetic shielding. However, for molecules with connected rings and complex three-dimensional structures, no reliable means to quantify the current strengths have existed so far.

In the present work, we use current-density calculations to determine the induced currents in benzene. The strength of the ring current is obtained by numerical integration of the net current through a bond cross section of one C–C bond. The calculations were performed at the HF-SCF and at various electron-correlated levels of theory using the TZP basis set. The obtained ring-current strengths are summarized in Table I. Electron-correlation effects on the ring-current

Downloaded 19 Aug 2004 to 128.146.233.123. Redistribution subject to AIP license or copyright, see http://jcp.aip.org/jcp/copyright.jsp

TABLE I. The strength of the induced ring current (current susceptibility, in nA T^{-1}) in benzene and the positive current contribution at the center oxygen in ozone calculated at different levels of theory using the TZP basis set.

Level	Benzene	Ozone
HF-SCF	12.81	225.89
DFT-BP86	11.41	23.23
MP2	12.04	145.21
CCSD	11.79	107.35
CCSD(T)	11.43	93.99
CCSDT		100.85
ARCS[a]	8.0	

[a]See Ref. 41.

strength in benzene amount to about 10%. At the CCSD(T) level, we obtain a net current strength of 11.4 nA T^{-1} as compared to the previous ARCS estimate of 8.0 nA T^{-1}.

In Fig. 3(a), the current-vector field in the molecular plane is shown for the case of a perpendicular magnetic field. In Fig. 3(b), a similar plot of the current-vector field for a plane 1 bohr above the molecular plane is displayed. It can be seen that the net current in the molecular plane is essentially zero, while in the plane 1 bohr above the ring, a net current is clearly visible. This means that the ring current is induced in the "π-electron cloud" and that significantly less current is flowing along the σ-bond framework.

C. Ozone

Ozone was chosen as an example for a molecule for which an accurate electron-correlation treatment is of great importance for a proper determination of the wave function. Although it is a particularly difficult system that is unusually badly described by single-reference methods, accurate nuclear magnetic shieldings have been obtained at the CCSDT level.[17] Due to the correspondence between nuclear magnetic shieldings and current densities, we are thus confident that the current density in ozone is also reasonably well described at the CCSDT level. Figure 4 shows the magnitude and the directions of the induced current density in ozone. When comparing the current density obtained at the CCSDT level with those calculated at the HF-SCF level, it is immediately obvious that for O_3 the current density is strongly affected by the electron-correlation effects. At the HF-SCF level, the circulation around the central oxygen is found to be significantly weaker as compared to the current density calculated at the CCSDT level. Similar comparisons of current densities calculated at the the MP2, CCSD, CCSD(T), and DFT levels reveal that the qualitative picture is correct at these levels of theory, but there are though substantial differences in the current densities around the nuclei, especially in the vicinity of the central oxygen.

D. Hexabenzocoronene

Hexabenzocoronene ($C_{42}H_{18}$) is a planar molecule consisting of 13 fused benzene rings belonging to the D_{6h} point group. Hexabenzocoronene has been chosen here to represent large molecules in order to show the applicability of current-density calculations to both larger and more complicated molecules with connected rings. Since each of the

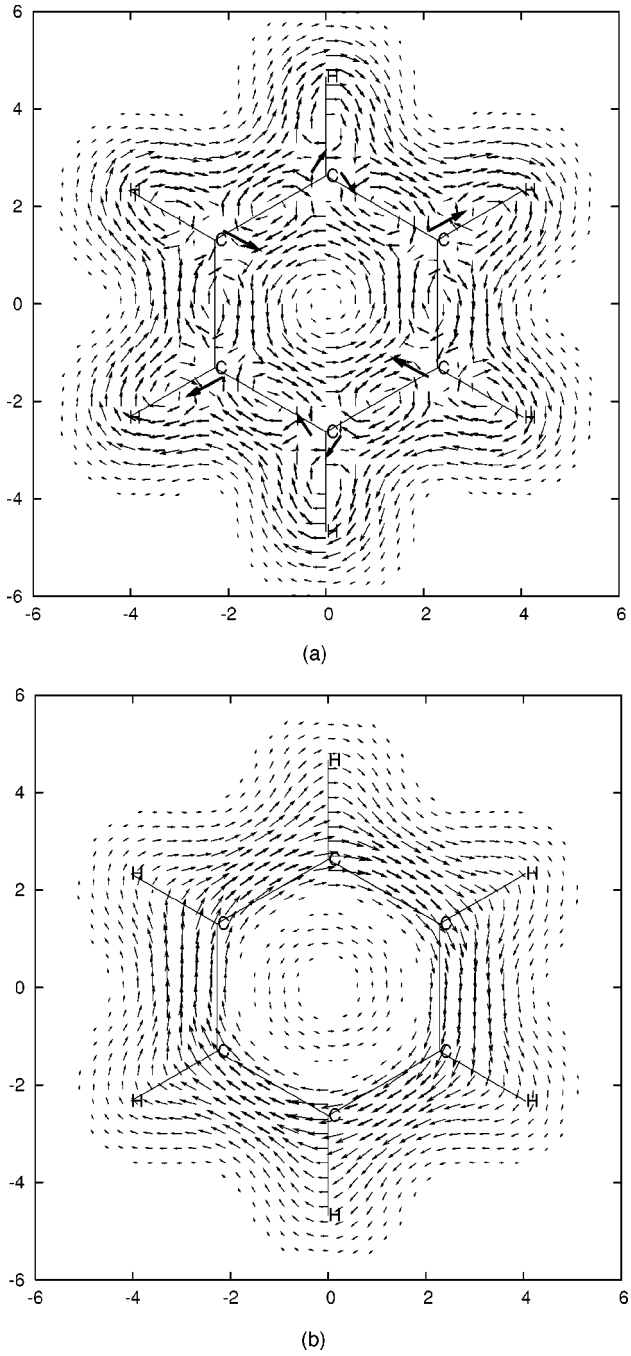

FIG. 3. The induced current density in benzene calculated at the HF-SCF/TZP level. (a) The current density in the plane defined by the nuclei, and (b) 1 bohr above the molecular plane with the magnetic field chosen perpendicular to the molecular plane.

fused benzene rings in $C_{42}H_{18}$ could in principle carry its own ring-current, it is not obvious which pathway the overall current actually takes and how strong are the net currents in the bonds of the molecule. The current density for $C_{42}H_{18}$ calculated at the DFT-BP86/SVP level is shown in Fig. 5. In Fig. 5(a), the current density calculated in a plane 1 bohr above the molecular framework is shown. The calculations clearly show that preferred aromatic pathways exist. This is seen even more clearly in Fig. 5(b), which shows the modulus of the current 1 bohr above the molecular plane. The calculations show the main current pathways; one around the

Downloaded 19 Aug 2004 to 128.146.233.123. Redistribution subject to AIP license or copyright, see http://jcp.aip.org/jcp/copyright.jsp

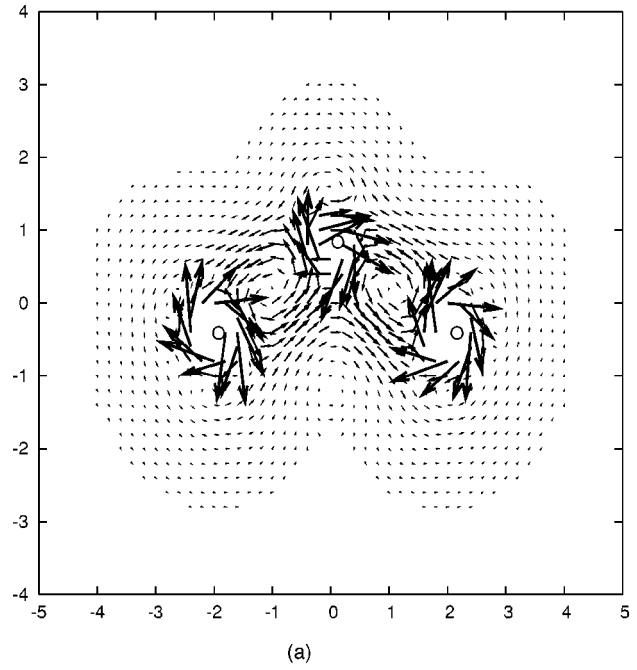

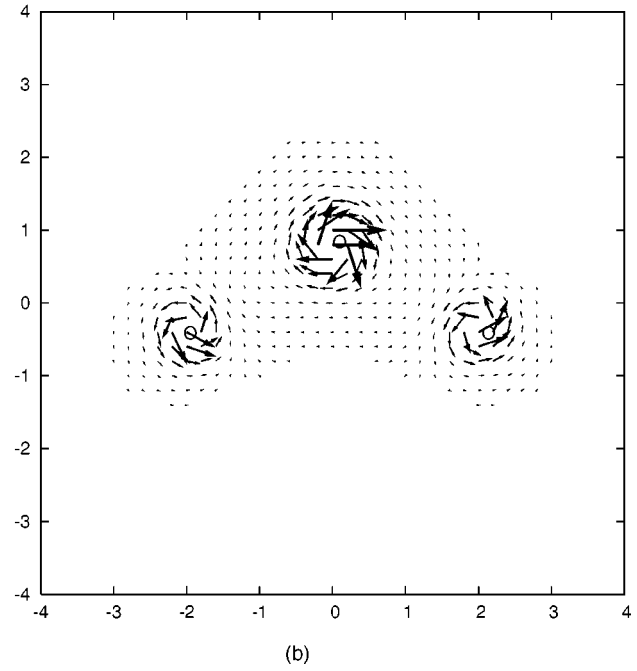

FIG. 4. The induced currents for ozone calculated at the CCSDT/TZP level (a) and the difference in the currents obtained at the CCSDT/TZP and HF-SCF/TZP levels (b). The currents are displayed in the plane containing the nuclei with the magnetic field chosen perpendicular to this plane.

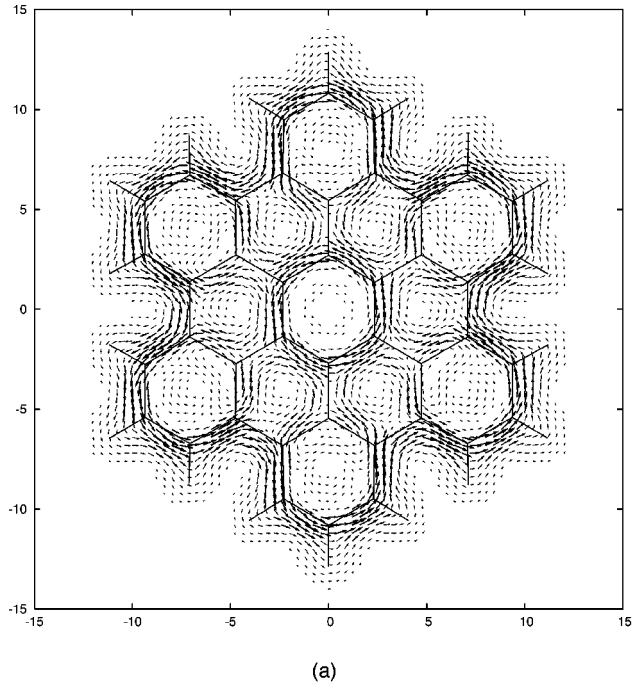

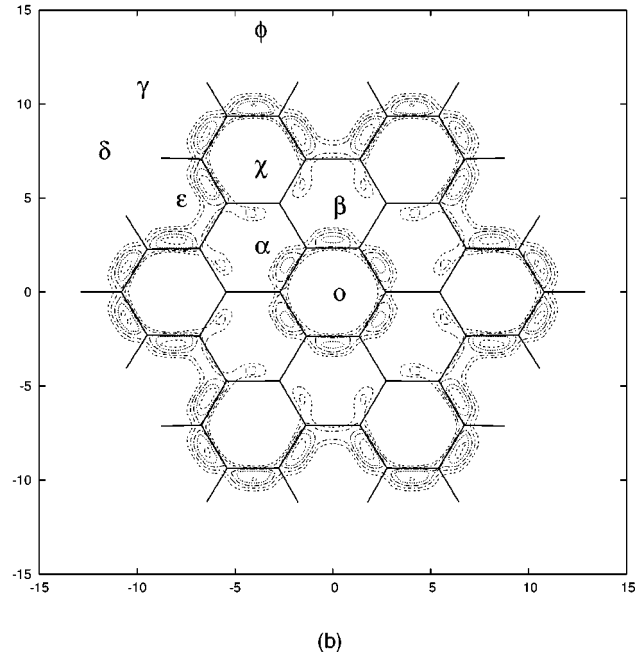

FIG. 5. The induced current density (a) and the modulus of the current density (b) for hexabenzocoronene calculated at the DFT-BP86/TZP level. The current density is displayed in a plane parallel to the molecular framework and 1 bohr above it with the magnetic field chosen perpendicular to the molecular plane. The symbols are used to define the cut planes for the numerical integration of the currents.

central benzene ring, and another is along the outer edges of the molecule. The main current pathways conform to Hückels $4n+2$ π-electron rule. The smaller paths having six π-electrons and the large path involves 30 π-electrons.

The current-density plots does not provide any accurate information about the absolute current strengths and how strong they are as compared to the current strengths in benzene, i.e., they do not provide any quantitative measure of the degree of aromaticity of $C_{42}H_{18}$.[73] In order to quantify the current strength in the different bonds, the current density passing the cut plane at the center of the bond and perpendicular to the bond was integrated numerically. The rings of the benzo groups [cut-plane through χ–δ in Fig. 5(b)] sustain an individual current of 7.5 nA T^{-1}. The current strength along the molecular edge (α–δ) around the whole molecule is 7.7 nA T^{-1} yielding a total current of about 15 nA T^{-1} in the outer half (χ–ϵ) of the benzo groups. The benzene ring at the molecular center ($o-\alpha$) sustains a current of 13.5 nA T^{-1}. These values were calculated at the HF-SCF/

Downloaded 19 Aug 2004 to 128.146.233.123. Redistribution subject to AIP license or copyright, see http://jcp.aip.org/jcp/copyright.jsp

TABLE II. The strength of the induced ring current (current susceptibility, in nA T^{-1}) in C–C bonds for hexabenzocoronene calculated at the HF-SCF/TZP and DFT-BP86/TZP levels using the RI-DFT-BP86/SVP structure.

Bond	HF-SCF/TZP	DFT-BP86/TZP
$o-\alpha$	13.46	10.93
$\alpha-\beta$	0.00	0.00
$\alpha-\chi$	−7.50	−7.69
$\alpha-\delta$	7.74	6.30
$\chi-\epsilon$	15.48	12.91
$\chi-\gamma$	−14.96	−12.30
$o-\delta$	21.20	17.22
$\alpha-\phi$	7.47	4.64

TZP level. The corresponding currents obtained at the DFT-BP86/TZP level are somewhat smaller. The net current strengths are summarized in Table II.

E. Porphin

Free-base porphyrin or porphin ($C_{20}N_4H_{14}$) consists of four pyrrolic rings connected by conjugated bonds to form a macro cycle. The aromaticity and the aromatic pathways of porphyrins have been subject to numerous studies.[42,74–80] In this work, we have calculated both the induced current density and the current strength in the different bonds of porphin at the DFT-BP86/TZVP level. See Table III. The induced currents in porphin (with the magnetic field perpendicular to the molecular plane) 1 bohr above the molecular framework is shown in Fig. 6. In the figure, it can be seen that the most preferential path for the current is on the ''back side'' of pyrrole units with an inner hydrogen atom and on the ''inside'' of pyrrole units lacking the inner hydrogen. The integrated values for the current also clearly shows this trend. For the pyrrolic ring with an inner hydrogen the ''back side'' current is 18.1 nA T^{-1}, whereas the inside current is only 8.2 nA T^{-1}. The corresponding values for the pyrrolic ring without the inner hydrogen are 12.0 and 14.0 nA T^{-1}, respectively. The total aromatic path is thus clearly a superposition of several aromatic pathways fulfilling the $4n+2$ Hückel rule. An interesting feature of this phenomenon is the additivity of the currents in the conjugated bridges which have an integrated current of 25.9 nA T^{-1}, which is the sum of the inner and outer currents in the pyrrole units.

F. Current conservation

Calculations of the divergence for H_2 and CO_2 at the HF-SCF/SVP level showed that the divergence of the current

TABLE III. The strength of the induced ring current (current susceptibility, in nA T^{-1}) in C–C and C–N bonds for porphin calculated at the DFT-BP86/TZVP level using the RI-DFT-BP86/SVP structure.

Bond	DFT-BP86/TZVP
$\alpha-\beta$	18.12
$\epsilon-\phi$	25.89
$\delta-\chi$	12.04
$\alpha-\epsilon$	8.20
$\epsilon-\chi$	13.95

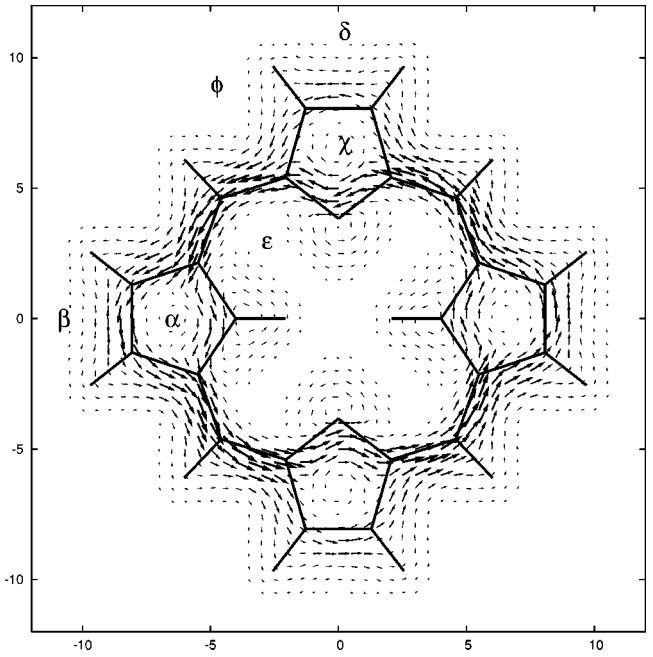

FIG. 6. The induced current density for porphin calculated at the DFT-BP86/TZVP level. The current is displayed in a plane parallel to the molecular framework and 1 bohr above it with the magnetic field chosen perpendicular to the molecular plane. The symbols are used to define the cut planes for the numerical integration of the currents.

significantly deviates from zero in the vicinity of the nuclei, and in regions where the current direction changes rapidly. By systematically augmenting the basis sets with functions of higher l-quantum numbers, the divergence slowly converges toward small values even close to the nuclei [see Figs. 7(b) and 7(c)]. For H_2, the use of a basis set of cc-pV5Z quality reduces the maximum value of the divergence to a value which is for all practical purposes equal to zero. The same quality basis for CO_2 still yields nonzero divergence near the nuclei. Discouraging as this may seem, a corresponding HF-SCF/SVP calculation without GIAOs and with the gauge origin at the carbon atom yields a maximum value of the divergence which is more than factor of 15 times larger than the largest divergence of the GIAO calculation. In the conventional calculation, the divergence also has a much broader spatial distribution. The effect of the GIAOs on the divergence can clearly be seen in Figs. 7(a) and 7(b). However, judging the magnitude of the divergence is not always easy. Therefore, one has to examine other properties of the current to be able to evaluate the quality of the results. The difference in the currents calculated at the HF-SCF/SVP and HF-SCF/cc-pV5Z levels is found to be small [see Figs. 1, 8(a), and 8(b)].

Also, by studying the convergence of the integrated current through a bond, one finds that induced current only changes by few percent when increasing the basis-set size from SVP to cc-pV5Z. At the HF-SCF level, the integrated value for the current passing half of the bond in CO_2 decreases from 10.03 to 9.81 nA T^{-1} when increasing the basis-set size from SVP to cc-pV5Z. For noncyclic molecules, for which the symmetry does not constrain the total

Downloaded 19 Aug 2004 to 128.146.233.123. Redistribution subject to AIP license or copyright, see http://jcp.aip.org/jcp/copyright.jsp

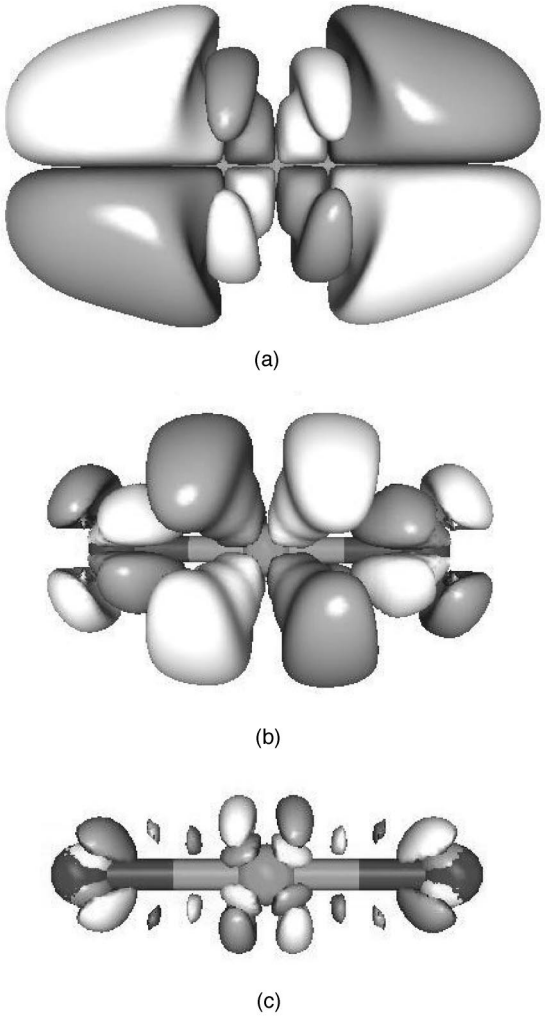

FIG. 7. The divergence of the current in CO_2 obtained in a conventional HF-SCF/SVP calculation (a). The corresponding divergence plots obtained at the GIAO HF-SCF/SVP and the GIAO HF-SCF/cc-pV5Z levels are depicted in (b) and (c), respectively. The iso-surfaces have been drawn to encompass any divergence larger than 0.01.

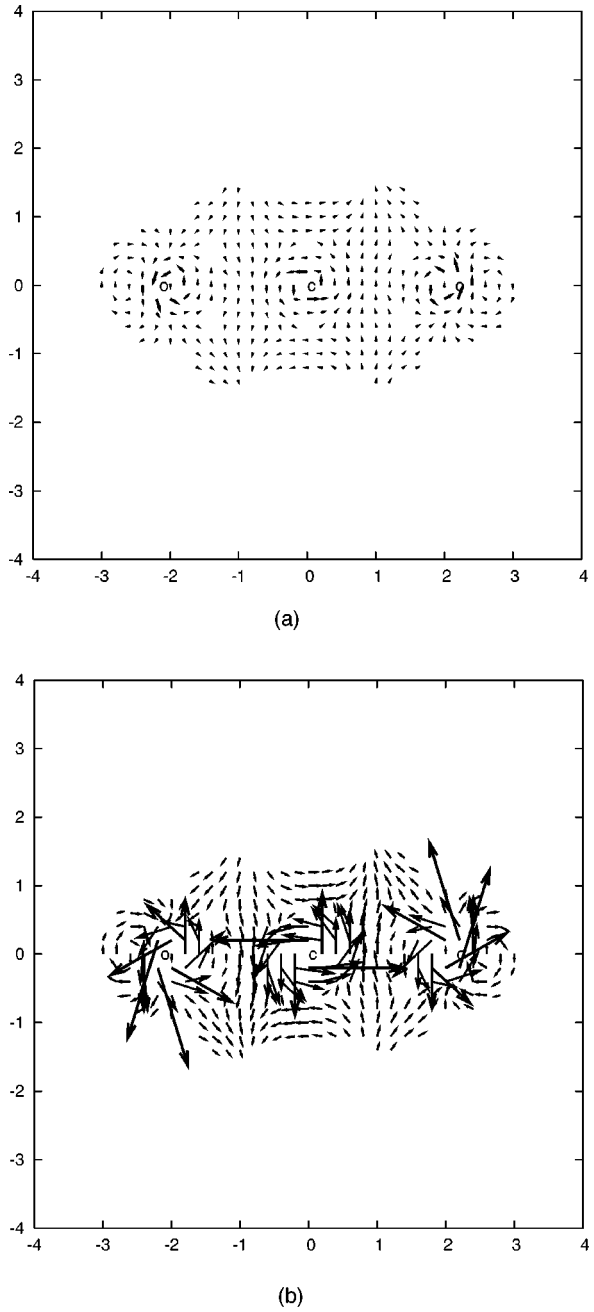

FIG. 8. The difference between induced current in CO_2 obtained using the SVP and cc-pV5Z basis sets (a), and the same figure enlarged ten times in (b).

current to be zero, the effects of the nonzero divergence can be seen more clearly. In water and ozone, which belong to the C_{2v} point group, the integrated current through the symmetry plane is particularly hard to converge to zero, because the cut plane goes through a nucleus where the divergence is large. For water, the difference between positive and negative current contributions calculated at the HF-SCF/SVP level is 0.68 nA T^{-1} as compared to the individual contributions of 24.67 and -23.99 nA T^{-1}, respectively. The corresponding values obtained in a HF-SCF/cc-pV5Z calculation are 0.0002, 23.4171, and -23.4169 nA T^{-1}, respectively.

By evaluating the Sambe–Epstein condition in Eq. (27) separately for each tensor component, one can estimate the total current leakage. At the HF-SCF/SVP level, the total leakage of the xy and yx components of the current tensor is -3.95 and 2.45 nA T^{-1}, respectively, whereas at the HF-SCF/cc-pV5Z level, the corresponding values are -0.2295 and 0.0044 nA T^{-1}. Thus, even though the divergence is not equal to zero in every point in space and the current leakage does not seem to be negligible, the integrated currents are well converged even when using fairly small standard basis sets.

V. SUMMARY AND OUTLOOK

We have presented a novel method for calculating magnetically induced current densities, and applied it to carbon dioxide, ozone, benzene, hexabenzocoronene, and porphin. Since GIAOs are used in the present approach, accurate current densities are in general obtained already with standard basis sets of SVP quality. The method thus opens the avenue to current-density calculations on large molecules of nanotechnological importance. In the current-density calculation,

Downloaded 19 Aug 2004 to 128.146.233.123. Redistribution subject to AIP license or copyright, see http://jcp.aip.org/jcp/copyright.jsp

the one-electron density matrices of magnetic shielding calculations and the basis-set information are the only references to the electron structure calculation implying that it is the magnetic shielding calculation that completely determines the applicability of the method; molecules with hundreds of atoms can be studied at the HF-SCF and DFT levels. The method can also be applied at any quantum chemical level of theory for which the one-electron density matrix and the one-electron perturbed density matrices are available. Current-density calculations at correlated levels are demonstrated here by DFT, MP2, CCSD, CCSD(T), and CCSDT calculations. To our knowledge, this is the first time molecular current densities have been calculated at electron-correlated levels of theory. Accurate current densities can also assist the development of new current-density functionals.[81]

Current-density plots can convey information about molecules, but such plots are not always too informative. Additional information about current strengths in bonds and current pathways in rings can be obtained by numerical integration of the current density passing selected cross sections in the molecule. The numerical integration provides values that can be used to quantify chemical concepts such as molecular aromaticity, electron delocalization, and molecular conductivity.

ACKNOWLEDGMENTS

We thank Professor Reinhart Ahlrichs (Karlsruhe) for an up-to-date version of the TURBOMOLE program package. Furthermore, we acknowledge support from the European research training network on ''Molecular Properties and Molecular Materials'' (MOLPROP), contract No. HPRN-2000-00013, from ''The Academy of Finland,'' the BMBF ''Zentrum für multifunktionelle Werkstoffe und miniaturisierte Funktionseinheiten,'' and from the ''Fonds der Chemischen Industrie.'' We would also like to thank Waldemar von Frenkells stiftelse and Magnus Ehrnrooths stiftelse for their generous support.

[1] J. Gauss and J. F. Stanton, Adv. Chem. Phys. **123**, 355 (2002).
[2] J. Gauss, K. Ruud, and T. Helgaker, J. Chem. Phys. **105**, 2804 (1996).
[3] F. London, J. Phys. Radium **8**, 397 (1937).
[4] H. Hameka, Mol. Phys. **1**, 203 (1958).
[5] R. Ditchfield, Mol. Phys. **27**, 789 (1974).
[6] K. Wolinski, J. F. Hinton, and P. Pulay, J. Am. Chem. Soc. **112**, 8251 (1990).
[7] P. Pulay, J. F. Hinton, and K. Wolinski, in *Nuclear Magnetic Shieldings and Molecular Structure*, edited by J. A. Tossell, NATO ASI Series C (Kluwer, Dordrecht, 1993), Vol. 386, p. 243.
[8] J. Gauss, Chem. Phys. Lett. **191**, 614 (1992).
[9] M. Häser, R. Ahlrichs, H. P. Baron, P. Weis, and H. Horn, Theor. Chim. Acta **83**, 551 (1992).
[10] K. Ruud, T. Helgaker, R. Kobayashi, P. Jørgensen, K. L. Bak, and H. J. A. Jensen, J. Chem. Phys. **100**, 8178 (1994).
[11] J. R. Cheeseman, G. W. Trucks, T. A. Keith, and M. J. Frisch, J. Chem. Phys. **104**, 5497 (1996).
[12] J. Gauss, J. Chem. Phys. **99**, 3629 (1993).
[13] J. Gauss and J. F. Stanton, J. Chem. Phys. **102**, 251 (1995).
[14] J. Gauss and J. F. Stanton, J. Chem. Phys. **104**, 2574 (1996).
[15] J. Gauss, Chem. Phys. Lett. **229**, 198 (1994).
[16] J. Gauss and J. F. Stanton, Phys. Chem. Chem. Phys. **2**, 2047 (2000).
[17] J. Gauss, J. Chem. Phys. **116**, 4773 (2002).
[18] A. M. Lee, N. C. Handy, and S. M. Colwell, J. Chem. Phys. **103**, 10095 (1995).
[19] G. Schreckenbach and T. Ziegler, J. Phys. Chem. **99**, 606 (1995).
[20] G. Rauhut, S. Puyear, K. Wolinski, and P. Pulay, J. Phys. Chem. **100**, 6310 (1996).
[21] D. B. Chesnut and C. K. Foley, Chem. Phys. Lett. **118**, 316 (1985).
[22] D. B. Chesnut and K. D. Moore, J. Comput. Chem. **10**, 648 (1985).
[23] M. Kallay and J. Gauss, J. Chem. Phys. **120**, 6841 (2004).
[24] T. Helgaker, M. Jaszunski, and K. Ruud, Chem. Rev. (Washington, D.C.) **99**, 293 (1999).
[25] P. Pulay, in *Modern Electronic Structure Theory*, edited by D. R. Yarkony (World Scientific, Singapore, 1995), Vol. 2, p. 1191.
[26] P. Lazzeretti, Prog. Nucl. Magn. Reson. Spectrosc. **36**, 1 (2000).
[27] P. Lazzeretti, in *Encyclopedia of Computational Chemistry*, edited by P. von Ragué Schleyer, N. L. Allinger, T. Clark, J. Gasteiger, P. A. Kollman, H. F. Schaefer III, and P. R. Schreiner (Wiley, New York, 1998), Vol. 3, p. 1659.
[28] T. A. Keith and R. F. W. Bader, Chem. Phys. Lett. **210**, 223 (1993).
[29] R. F. W. Bader and T. A. Keith, J. Chem. Phys. **99**, 3683 (1993).
[30] P. Lazzeretti, M. Malagoli, and R. Zanasi, Chem. Phys. Lett. **220**, 299 (1994).
[31] S. Coriani, P. Lazzeretti, M. Malagoli, and R. Zanasi, Theor. Chim. Acta **89**, 181 (1994).
[32] R. Zanasi, P. Lazzeretti, M. Malagoli, and F. Piccinini, J. Chem. Phys. **102**, 7150 (1995).
[33] R. Zanasi, J. Chem. Phys. **105**, 1460 (1996).
[34] P. W. Fowler, R. Zanasi, B. Cadioli, and E. Steiner, Chem. Phys. Lett. **251**, 132 (1996).
[35] R. Zanasi and P. Lazzeretti, Mol. Phys. **92**, 609 (1997).
[36] P. W. Fowler, E. Steiner, B. Cadioli, and R. Zanasi, J. Phys. Chem. A **102**, 7297 (1998).
[37] A. Ligabue, S. P. A. Sauer, and P. Lazzeretti, J. Chem. Phys. **118**, 6830 (2003).
[38] F. R. Salsbury, Jr. and R. A. Harris, J. Chem. Phys. **104**, 5497 (1996).
[39] J. A. Elvidge and L. M. Jackman, J. Chem. Soc. 859 (1961).
[40] J. A. Pople and K. G. Untch, J. Am. Chem. Soc. **88**, 4811 (1966).
[41] J. Jusélius and D. Sundholm, Phys. Chem. Chem. Phys. **1**, 3429 (1999).
[42] J. Jusélius and D. Sundholm, Phys. Chem. Chem. Phys. **2**, 2145 (2000).
[43] J. Jusélius and D. Sundholm, J. Org. Chem. **65**, 5233 (2000).
[44] J. Jusélius and D. Sundholm, Phys. Chem. Chem. Phys. **3**, 2433 (2001).
[45] J. Jusélius, M. Straka, and D. Sundholm, J. Phys. Chem. A **105**, 9939 (2001).
[46] R. J. F. Berger, M. A. Schmidt, J. Jusélius, D. Sundholm, P. Sirsch, and H. Schmidbaur, Z. Naturforsch., B: Chem. Sci. **56**, 979 (2001).
[47] J. Jusélius, M. Patzschke, and D. Sundholm, J. Mol. Struct.: THEOCHEM **633**, 123 (2003).
[48] In the complete basis-set limit, gauge invariance is ensured for variational schemes such as HF-SCF and multiconfigurational SCF, but gauge-invariance is not achieved for nonvariational approaches within CC framework (for a detailed discussion see, for example, Ref. 82).
[49] A. E. Hansen and T. D. Bouman, in Ref. 7, p. 117.
[50] W. Kutzelnigg, C. van Wüllen, U. Fleischer, R. Franke, and T. van Mourik, in *Nuclear Magnetic Shieldings and Molecular Structure*, edited by J. A. Tossell (Kluwer Academic, Dordrecht, 1993), pp. 141–161.
[51] *Handbook of Mathematical Functions* edited by M. Abramowitz and I. A. Stegun (Dover, New York, 1965).
[52] S. T. Epstein, J. Chem. Phys. **58**, 1592 (1973).
[53] T. H. Dunning, Jr., J. Chem. Phys. **90**, 1007 (1989).
[54] A. Schäfer, H. Horn, and R. Ahlrichs, J. Chem. Phys. **97**, 2571 (1992).
[55] R. Ahlrichs, M. Bär, M. Häser, H. Horn, and C. Kölmel, Chem. Phys. Lett. **162**, 165 (1989), current version: see http://www.turbomole.de
[56] D. E. Woon and T. H. Dunning, Jr., J. Chem. Phys. **103**, 4572 (1995).
[57] K. Eichkorn, O. Treutler, H. Öhm, M. Häser, and R. Ahlrichs, Chem. Phys. Lett. **240**, 283 (1995).
[58] S. H. Vosko, L. Wilk, and M. Nusair, Can. J. Phys. **58**, 1200 (1980).
[59] J. P. Perdew, Phys. Rev. B **33**, 8822 (1986).
[60] A. D. Becke, Phys. Rev. A **38**, 3098 (1988).
[61] A. Schäfer, C. Huber, and R. Ahlrichs, J. Chem. Phys. **100**, 5829 (1994).
[62] J. F. Stanton, J. Gauss, J. D. Watts, W. J. Lauderdale, and R. J. Bartlett, Int. J. Quantum Chem., Quantum Chem. Symp. **26**, 879 (1992), current version: see http://www.aces2.de

Downloaded 19 Aug 2004 to 128.146.233.123. Redistribution subject to AIP license or copyright, see http://jcp.aip.org/jcp/copyright.jsp

[63] Chem. Rev. (Washington, D.C.) **101**, (2001), aromaticity is the theme of issue 5.
[64] E. D. Jemmis and P. von Ragué Schleyer, J. Am. Chem. Soc. **104**, 4781 (1982).
[65] L. Pauling, J. Chem. Phys. **4**, 673 (1936).
[66] J. A. Pople, J. Chem. Phys. **24**, 1111 (1956).
[67] J. A. Pople, Mol. Phys. **1**, 175 (1958).
[68] R. McWeeny, Mol. Phys. **1**, 311 (1958).
[69] V. I. Minkin, M. N. Glukhovtsev, and B. Y. Simkin, *Aromaticity and Antiaromaticity-Electronic and Structural Aspects* (Wiley, New York, 1994).
[70] U. Fleischer, W. Kutzelnigg, P. Lazzeretti, and V. Mühlenkamp, J. Am. Chem. Soc. **116**, 5298 (1994).
[71] M. Bilde and A. Hansen, Mol. Phys. **92**, 237 (1997).
[72] I. Morao and F. P. Cossío, J. Org. Chem. **64**, 1868 (1999).
[73] A. Soncini, E. Steiner, P. W. Fowler, R. W. A. Havenith, and L. W. Jenneskens, Chem.-Eur. J. **9**, 2974 (2003).
[74] M. K. Cyrañski, T. M. Krygowski, M. Wisiorowski, N. J. R. van Eikema Hommes, and P. von Ragué Schleyer, Angew. Chem., Int. Ed. Engl. **37**, 177 (1998).
[75] D. Lloyd, J. Chem. Inf. Comput. Sci. **36**, 442 (1996).
[76] E. Vogel, W. Haas, B. Knipp, J. Lex, and H. Schmickler, Angew. Chem., Int. Ed. Engl. **27**, 406 (1988).
[77] E. Vogel, J. Heterocycl. Chem. **33**, 1461 (1996).
[78] T. D. Lash and S. T. Chaney, Chem.-Eur. J. **2**, 944 (1996).
[79] T. D. Lash, J. L. Romanic, J. Hayes, and J. D. Spence, Chem. Commun. (Cambridge) 819 (1999).
[80] E. Steiner and P. W. Fowler, ChemPhysChem **3**, 114 (2002).
[81] G. Vignale and W. Kohn, Phys. Rev. Lett. **77**, 2037 (1996).
[82] T. B. Pedersen and H. Koch, J. Chem. Phys. **106**, 8059 (1997).

Downloaded 19 Aug 2004 to 128.146.233.123. Redistribution subject to AIP license or copyright, see http://jcp.aip.org/jcp/copyright.jsp